

## The Secretory Portal- Porosome in Pancreatic Acinar Cells

Bhanu P. Jena

Department of Physiology, Wayne State University School of Medicine, Detroit, MI 48201, USA.

e-mail: [bjena@med.wayne.edu](mailto:bjena@med.wayne.edu)

Version 1.0, February 26, 2014 [DOI: 10.3998/panc.2014.2]

### 1. Introduction

While it is believed that secretory vesicles completely merge with the cell plasma membrane during secretion resulting in release of the entire vesicular contents, the observation of partially empty vesicles in cells following secretion (**Figure 1**), is incompatible with complete vesicle merger, suggesting the presence of an additional mechanism involving transient fusion that allows partial discharge of intra-vesicular contents during secretion. In 1973, the mechanism of ‘transient’ or ‘kiss-and-run’ mechanism of secretory vesicle fusion at the cell plasma membrane enabling fractional release of intravesicular contents was proposed (7). Then in 1990 it was hypothesized that the fusion pore, a continuity established between the vesicle membrane and the cell plasma membrane, results from a “preassembled ion channel-like structure that could open and close” (2). A later 1992 review opined that the principal difficulty in observing these structures and fusion pore formation at these structures, was the lack of ultrahigh resolution imaging tools to directly monitor their presence and study their activity in live cells (4).

In the mid 1990’s, employing the then newly developed technique of atomic force microscopy (AFM), nanometer scale pore structures and their dynamics were discovered at the apical plasma membrane in live pancreatic acinar cells. Circular pit-like structures containing 100-180 nm cup-shaped depressions or pores were observed at the apical plasma membrane of pancreatic acinar

cells where secretion is known to occur (57). During secretion, the depressions or pores opening grew larger, returning to their resting size following completion of cell secretion.

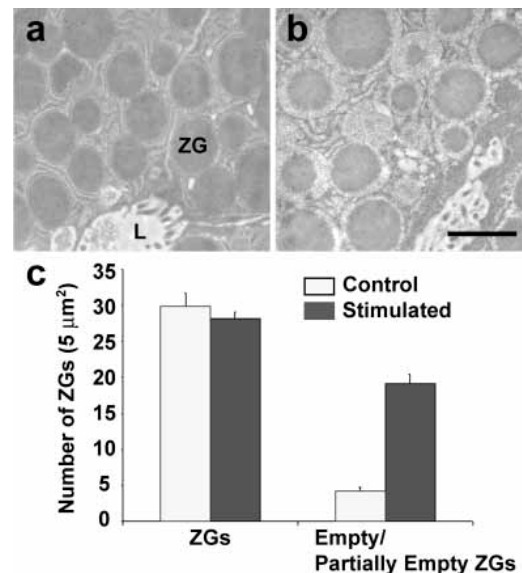


**Figure 1.** Representative electron micrographs of resting (a), and cholecystokinin-stimulated for 15 min (b) rat pancreatic acinar cells, demonstrating partial loss of zymogen granule (ZG) contents following secretion. The apical lumen (L) of acini demonstrating the presence of microvilli and secreted products is observed. (c) These studies using electron microscopy further demonstrate that while the number of ZG remain unchanged following secretion, an increase in the number of empty and partially empty vesicles are observed. Scale bar = 1 μm (From Ref 10).

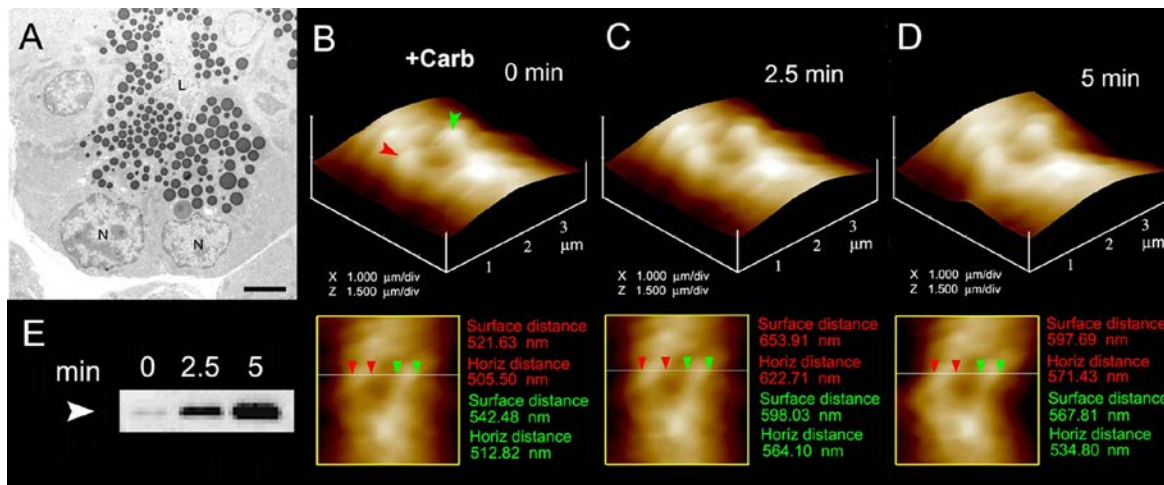


**Figure 2.** The volume dynamics of zymogen granules (ZG) in live pancreatic acinar cells demonstrating fractional release of ZG contents during secretion. **(A)** Electron micrograph of pancreatic acinar cells showing the basolaterally located nucleus (N) and the apically located electron-dense vesicles, the ZGs. The apical end of the cell faces the acinar lumen (L). Bar = 2.5  $\mu\text{m}$ . **(B-D)** Apical ends of live pancreatic acinar cells in physiological buffer imaged by AFM, showing ZGs (red and green arrowheads) lying just below the apical plasma membrane. Exposure of the cell to a secretory stimulus (1  $\mu\text{M}$  carbamylcholine), results in ZG swelling within 2.5 min, followed by a decrease in ZG size after 5 min. The decrease in size of ZGs after 5 min is due to the release of secretory products such as  $\alpha$ -amylase, as demonstrated by the immunoblot assay **(E)**. If ZG's had fused at the plasma membrane and fully merged, it would not be visible, demonstrating transient fusion and fractional discharge on intravesicular contents during secretion in pancreatic acinar cells (From Ref 42).

Studies next established the observed depressions to be the secretory portals at the plasma membrane in cells (13, 35). Following stimulation of cell secretion, gold-conjugated amylase antibodies (amylase being one of the major intra-vesicular enzymes secreted by pancreatic acinar cells) accumulate at depressions. These results established depressions to be the long sought-after secretory portals in cells. The study further reported the presence of t-SNAREs at the porosome base facing the cytosol, firmly establishing depression structures to be secretory portals where vesicles transiently dock and fuse for intra-vesicular content release during secretion (35). Subsequently depressions and their dynamics at the cell plasma membrane in growth hormone (GH) secreting cells of the pituitary gland, and in rat chromaffin cells was reported (15). In 2003, following immunoisolation of the depression structures from acinar cells of the exocrine pancreas, their composition was determined, and they were functionally reconstituted into artificial lipid membranes (40). Morphological details of

depressions associated with docked secretory vesicles were revealed using high-resolution electron microscopy (40). In the past decade, employing a combination of approaches such as AFM, biochemistry, electrophysiology, conventional EM, mass spectrometry, and small angle X-Ray solution scattering analysis, this specialized portal has been found to be present in all secretory cells examined, including neurons (18, 36, 43, 47). Therefore, these structures were named 'porosomes' (36, 43, 46) or secretory portals in cells. Our own studies and studies from other laboratories established porosomes to be secretory portals that perform the specialized task of fractional discharge of intravesicular contents from cells during secretion (20, 23, 26, 32, 36, 43, 46, 49, 52, 54, 56, 61). The significance of the identification of the porosome is reflected by several publications regarding the structure and the associated transient fusion mechanism by fractional discharge of intravesicular contents from cells (3, 20, 23, 26, 32, 49, 52, 54, 56, 61, 68, 69).

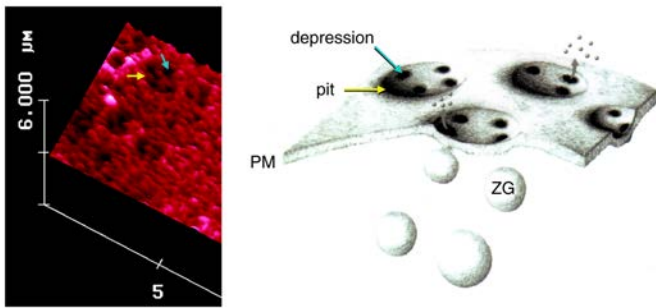


**Figure 3.** To the left is an AFM micrograph of the apical plasma membrane of a live pancreatic acinar cell demonstrating the presence of a pit (yellow arrow) with porosomes within (blue arrow). To the right is a schematic drawing demonstrating pits and cup-shaped porosomes where zymogen granules (ZG), the secretory vesicles in exocrine pancreas dock and transiently fuse to release intra-vesicular digestive enzymes from the cell (From Ref 57).

It has been demonstrated in exocrine, endocrine, and neuronal cells that “secretory granules are recaptured largely intact following stimulated exocytosis in cultured endocrine cells” (68); that “single synaptic vesicles fuse transiently and successively without loss of identity” (3); and that “zymogen granule exocytosis is characterized by long fusion pore openings and preservation of vesicle lipid identity” (44, 69). The past two decades have witnessed great progress in our understanding of  $\text{Ca}^{+2}$  and SNARE-mediated membrane fusion and on secretory vesicle volume regulation required for regulated fractional release of intravesicular contents from cells during secretion (4, 6, 8, 9, 12, 14, 16, 17, 19, 21, 24, 29-31, 34, 37, 38, 39, 41, 42, 45, 48, 50, 51, 55, 58, 59, 62, 64, 66, 70, 72-74). These findings have greatly contributed to the progress in our understanding of the involvement of porosomes in the secretory process.

## 2. Discovery of the Porosome

The porosome was first discovered in acinar cells of the rat exocrine pancreas nearly 17 years ago (57). This discovery was made possible by the use of a then new microscope, the atomic force microscope (AFM) (1,5). In AFM, a probe tip micro fabricated from silicon or silicon nitride and mounted on a cantilever spring is used to scan

the surface of the sample at a constant force. Either the probe or the sample can be precisely moved in a raster pattern using a xyz piezo to scan the surface of the sample. The deflection of the cantilever measured optically is used to generate an isoforce relief of the sample (5, 71). Force is thus used by the AFM to image surface profiles of objects at nanometer resolution and in real time, objects such as live cells, subcellular organelles, and even biomolecules, submerged in physiological buffer solutions.

Exocrine pancreatic acinar cells are polarized secretory cells possessing an apical and a basolateral end. Pancreatic acinar cells synthesize digestive enzymes, which are stored within 0.2-1.2  $\mu\text{m}$  in diameter apically located membranous sacs or secretory vesicles, called zymogen granules (ZGs). Following a secretory stimulus, ZGs dock and fuse with the apical plasma membrane to release their contents to the outside. As opposed to neurons where secretion of neurotransmitters occur within millisecond of a secretory stimulus, pancreatic acinar cells secrete digestive enzymes over several minutes following a stimuli, and therefore was chosen as a model system to dissect out the various steps involved in cell secretion. AFM studies of the structure and dynamics of the apical plasma membrane in both resting and stimulated live pancreatic acinar cells, demonstrate the presence of new cellular structures at the apical plasma membrane of the cell where secretion is known to occur (57). At the apical plasma membrane, a group of circular ‘pits’ measuring 0.4–1.2  $\mu\text{m}$  in diameter, contain smaller 100-180 nm in diameter ‘depressions’ structures are identified (**Figure 3**). Typically 3–4 depressions are found within each pit structure, and interestingly the basolateral cell membrane is devoid of such pit and depression structures (57). High-resolution AFM images of depressions in live acinar cells further reveal a cone-shaped basket-like morphology, each cone measuring 15–35 nm in depth. View of the porosome structure at the cytosolic compartment of the plasma membrane in the exocrine pancreas has also been determined at near nm resolution in live cells (**Figure 4**) (40). To determine the

morphology of porosomes at the cytosolic compartment in pancreatic acinar cells, isolated plasma membrane preparations in near physiological buffered solution, have been imaged at ultrahigh resolution using the AFM (**Figure 4**) (40). As demonstrated in the AFM surface topology study, study of inside-out acinar cell plasma membrane preparations reveal scattered circular disks (pits) measuring 0.5–1  $\mu\text{m}$  in diameter, with inverted cup-shaped structures (depressions or porosomes) within (40). On a number of occasions, ZGs ranging in size from 0.4–1  $\mu\text{m}$  in diameter are observed in association with one or more of the inverted cups, suggesting the circular disks to represent pits, and inverted cups porosomes (**Figure 4**) (40). Porosomes in acinar cells of the exocrine pancreas have also been examined using high-resolution transmission electron microscopy (TEM) (**Figures 5 and 6**), both in isolated cells and tissues (**Figure 5**), and in association with ZGs prepared from stimulated acinar cells (**Figure 6**) (20, 34, 39, 71). In Figure 5, the electron micrograph of a depression or porosome sectioned at a certain angle depicts its distinct and separate bilayer, and the bilayer attachment of the associated ZG. A cross section through three lateral knob-like

structures that circle around the porosome cup, are clearly delineated. The apical knob-like density at the lip of the porosome, appear most prominent. The TEM micrograph further demonstrates that the lower knob, likely represents the t-/v-SNARE ring or rosette complexes formed as a result of ZG membrane fusion at the base of the porosome.

Exposure of pancreatic acinar cells to a secretagogue results in a time-dependent increase (20–45%) in both the diameter and relative depth of depressions (**Figure 7**). Porosomes return to resting size on completion of cell secretion (13, 57). No demonstrable change in pit size is detected following stimulation of secretion (57). Enlargement of porosome diameter and an increase in its relative depth, following exposure to a secretagogue correlates with secretion (**Figure 7,8**). Additionally, exposure to cytochalasin B, a fungal toxin that inhibits actin polymerization and secretion, results in a 15–20% decrease in porosome size and a consequent 50–60% loss in cell secretion (57). These results suggested depressions or porosomes to be the secretory portals in pancreatic acinar cells.

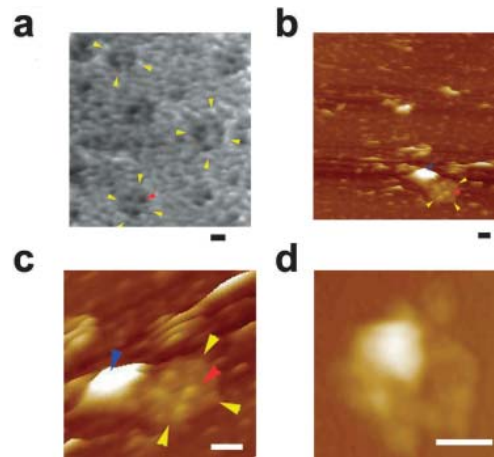


**Figure 4.** AFM micrograph showing cup-shaped depression or porosome structures at the pancreatic acinar cell plasma membrane. (a) Several circular “pits” (yellow arrowheads) with depressions or porosomes (red arrowheads) are seen in this AFM micrograph of the apical plasma membrane in live pancreatic acinar cell. (b) AFM micrograph of the cytosolic compartment of isolated pancreatic plasma membrane preparation depicting a “pit” (yellow arrowheads) containing several inverted cup-shaped porosomes (red arrowhead) within. ZG (blue arrowhead) is found associated with porosomes in figures c and d. (c) The “pit” and inverted fusion pores in b is shown at higher magnification. (d) AFM micrograph of another “pit” with inverted fusion pores within, and associated with a ZG, is shown. Bar = 200 nm. (From Ref 40).

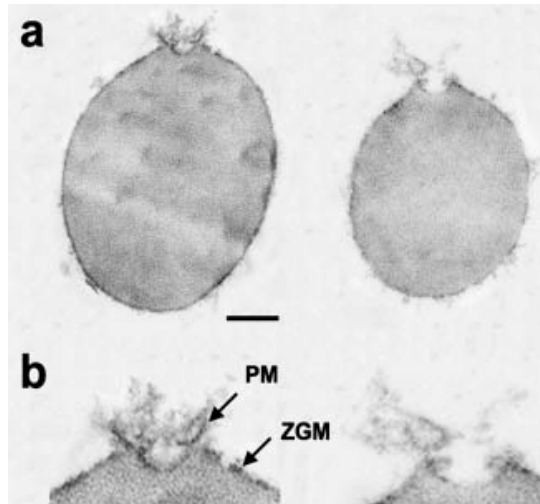


**Figure 5.** Transmission electron micrograph of a porosome associated with a docked secretory vesicle at the apical end of a pancreatic acinar cell. **(a)** Part of the apical end of a pancreatic acinar cell demonstrating within the green square, the presence of a porosome and an associated zymogen granule (ZG) fused at its base. (Bar=400 nm only in figure a). **(b)** The area within the green square in figure a, has been enlarged to show the apical microvilli (MV) and a section through the porosome and the ZG. Note the ZG membrane (ZGM) bilayer is fused at the base of the porosome cup. **(c)** A higher magnification the porosome-associated ZG shows in greater detail the porosome bilayer and cross section through the three protein rings (which appear as knobs in either side of the cup-shaped porosome), with the thicker ring (blue arrowhead) present close to the opening of the porosome to the outside, which may regulate the closing and opening of the structure. The third and the lowest ring away from the porosome opening is attached to the ZGM, and may represent the t-*v*-SNARE rosette or ring complex. **(d)** Yellow outline of the ZG fused porosome complex (FP) demonstrating the continuity with the apical plasma membrane (PM) at the apical end of the pancreatic acinar cell facing the lumen (L). The exact points of contact and fusion of the ZGM with the membrane at the porosome base is clearly seen in the micrograph. (From Ref 40).

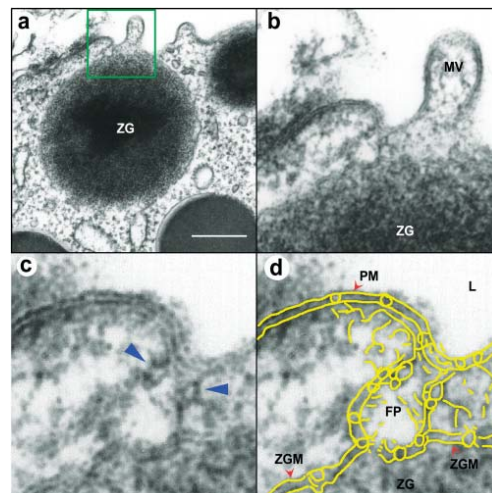


**Figure 6.** Transmission electron micrographs of zymogen granules (ZGs) co-isolated with porosomes. **(a)** Porosome associated at the surface of ZGs are shown. (Bar=120 nm; top panel only). **(b)** At higher magnification details of the porosome complex demonstrating the presence of separate plasma membrane (PM) and the ZG membrane (ZGM). Note the apically arranged ring complex of the porosome, similar to what is observed in electron micrographs of the structure in intact cells as presented in figure 5. These ZG-associated porosomes are torn off the cell plasma membrane and hence have very little membrane. Hence the porosome proteins lining the porosome cup appear as frills in the electron micrograph. Note the ZG size compared to the porosome structure. (From Ref 40).

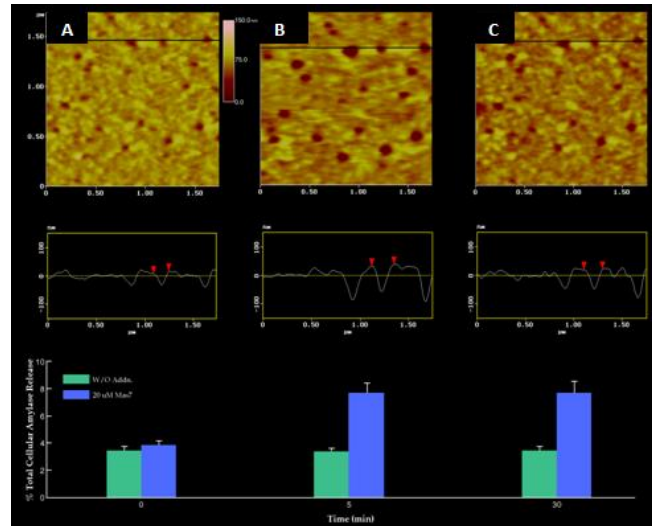


**Figure 7.** Dynamics of depressions following stimulation of secretion in live pancreatic acinar cell examined using AFM. (a) Several depressions within a pit are shown in the AFM micrographs. The scan line across three depressions in the top panel is represented graphically in the middle panel and defines the diameter and relative depth of three depressions; the depression to the center is labeled using red arrowheads. The bottom panel shows % total cellular amylase release in the presence (blue bars) and absence (green bars) of the secretagogue Mas7. (b) Note the increase in depression diameter and relative depth, correlating with an increase in total cellular amylase release at 5 min after stimulation of secretion. (c) At 30 min after stimulation, there is a decrease in diameter and depth of the depressions and no further increase in amylase release over the 5-min time point is seen. No significant changes in amylase secretion or depression diameter were observed in control acini, in either the presence or the absence of the non-stimulatory mastoparan analogue Mas17, throughout the times examined. High-resolution images of pits and their depressions were obtained before and after stimulation with Mas7, for up to 30 min (From Ref 57).

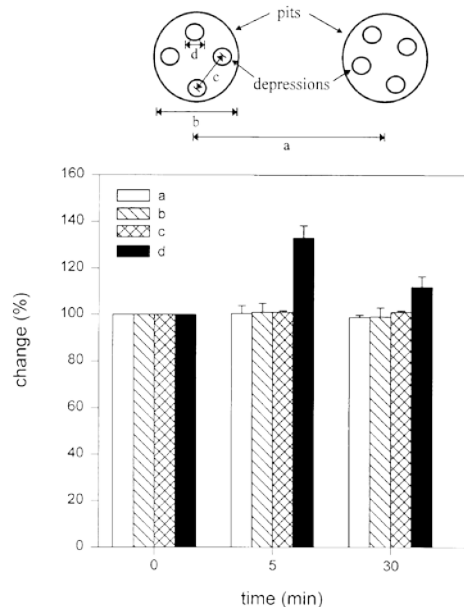


**Figure 8.** Changes are observed only in depressions or porosomes following stimulation of secretion. Analysis of the dimensions **a–d**, schematically represented at the top and graphically presented below, demonstrates a significant increase in the depression diameter at 5 min and a return toward prestimulatory levels after 30 min. No changes (100%) in **a–c** are seen throughout the times examined. Pit and depression diameters were estimated using section analysis software from Digital Instruments. Each single pit or depression was measured twice, once in the scan direction and once at 90° to the first (From Ref 57).

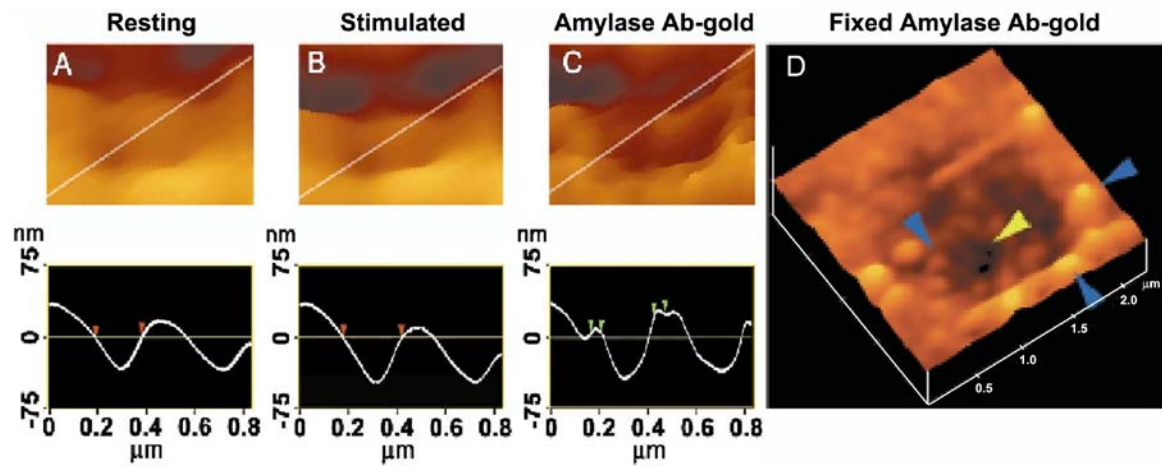


**Figure 9.** Intravesicular contents are expelled to the outside through the porosome during cell secretion. (A and B) AFM micrograph and section analysis of a pit and two of the four depressions or porosomes, demonstrating enlargement of porosomes following stimulation of cell secretion in the acinar cell of the exocrine pancreas. (C) Exposure of live cells to gold conjugated-amylase antibody (Ab) results in specific localization of gold particles to these secretory sites. Note the localization of amylase-specific 30 nm immunogold particles at the edge of porosomes. (D) AFM micrograph of pits and porosomes with immunogold localization demonstrated in cells immunolabeled and then fixed. Blue arrowheads point to immunogold clusters and the yellow arrowhead points to a depression or porosome opening. (From Ref 13).

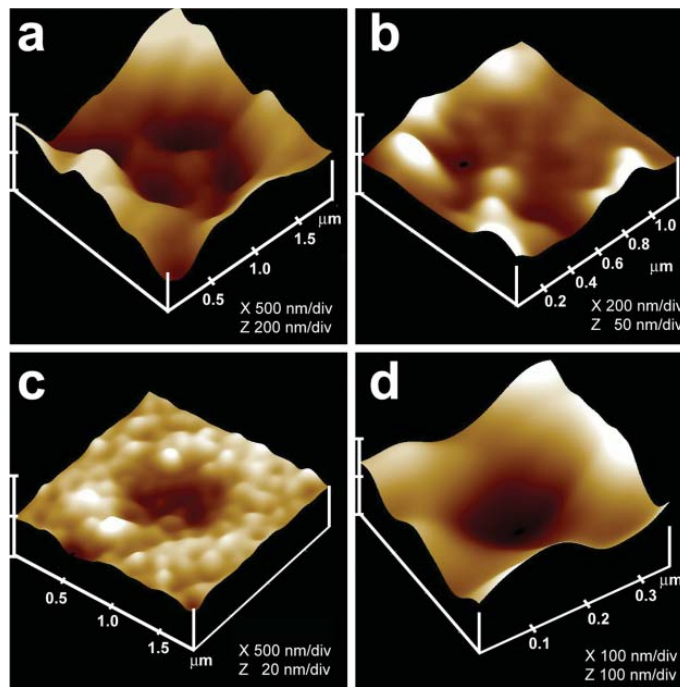


**Figure 10.** AFM and immune-AFM micrographs of the pancreatic acinar cell porosome demonstrating pore morphology and the release of secretory products at the site. (a) A pit with four porosomes within, found at the apical surface in a live pancreatic acinar cell; (b) After stimulation of secretion, amylase-specific immunogold localize at the pit and porosomes within, demonstrating them to be secretory release sites; (c) Some porosomes demonstrate greater immunogold localization, suggesting more release through them; (d) AFM micrograph of a single porosome in a live acinar cell (From Ref 35).

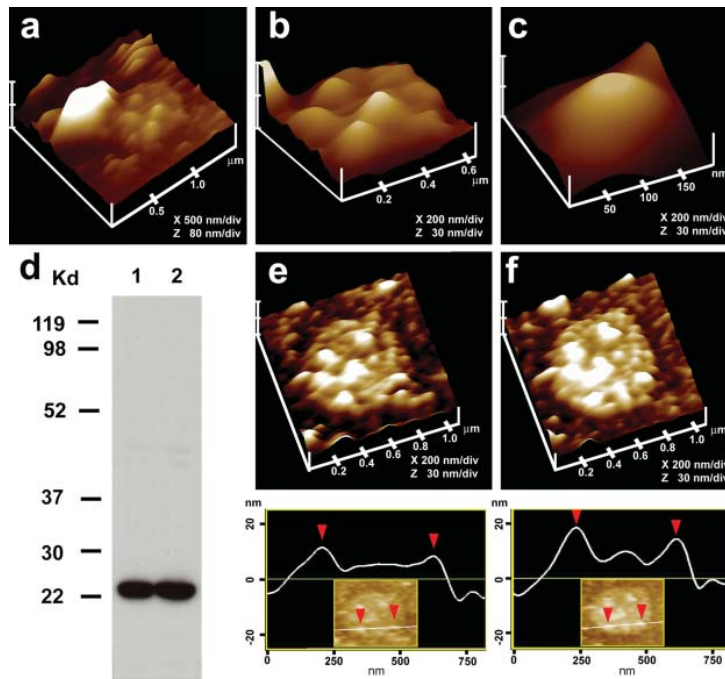


**Figure 11.** Immuno-AFM of the cytosolic compartment of the porosome complex demonstrate the presence of the t-SNARE SNAP-23 at the porosome base. (a) AFM micrograph of isolated plasma membrane preparation reveals the cytosolic compartment of a pit with inverted cup-shaped porosomes. Note the 600 nm in diameter docked ZG to the left. (b) Higher magnification of the same pit demonstrates the presence of 4–5 porosomes within. (c) A single porosome is depicted in this AFM micrograph. (d) Western blot analysis of 10 µg and 20 µg of pancreatic plasma membrane preparations using SNAP-23 antibody demonstrates a single 23 kDa immunoreactive band. (e and f) The cytosolic side of the plasma membrane demonstrates the presence of a pit with a number of porosomes within, shown before (e) and after (f) addition of the SNAP-23 specific antibody. Note the increase in height of the porosome base revealed by section analysis (bottom panel), demonstrating localization of SNAP-23 antibody to the base of the porosome (From Ref 35).

Results from these studies further demonstrate the involvement of actin in regulation of both the structure and function of porosomes. To further demonstrate porosomes to be secretory portals, required the direct observation of the release of secretory products through the structure. This was accomplished using immuno-AFM studies in exocrine pancreas (**Figure 9,10**) where gold-conjugated amylase-specific antibody was demonstrated to selectively localize at the mouth of depression or porosome opening to the cell exterior, following stimulation of secretion (13, 35).

To further confirm that the cup-shaped structures are porosomes, where secretory vesicles dock and fuse, additional immuno-AFM studies have been performed (35). Since ZGs dock and fuse at the plasma membrane to release vesicular

contents, it was hypothesized that if the inverted cups or porosomes are the secretory portals, then plasma membrane-associated t-SNAREs should localize at the structure. The t-SNARE protein SNAP-23 is present in pancreatic acinar cells (35). A polyclonal monospecific SNAP-23 antibody recognizing a single 23 kDa protein in Western blots of pancreatic plasma membrane fraction, when used in immuno-AFM studies, demonstrated selective localization to the base of the porosome (**Figure 11**) (35). These results establish that the inverted cup-shaped porosome structures in inside-out pancreatic plasma membrane preparations are indeed secretory portals where secretory vesicles transiently dock and fuse to release their contents during cell secretion.

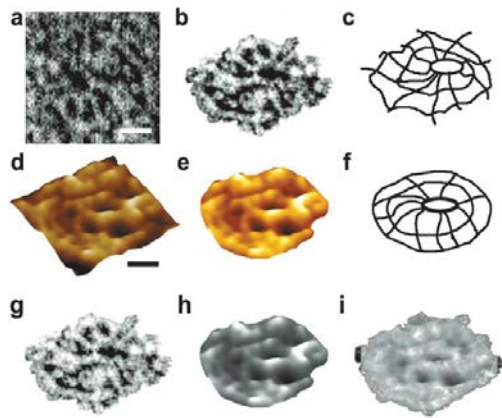


**Figure 12.** Negatively stained EM and AFM of the immunisolated porosome complex from exocrine pancreas. **(a)** Negatively stained EM of an immunisolated porosome complex from solubilized pancreatic plasma membrane preparation using a SNAP-23 specific antibody. Note the three rings and the 10 spokes that originate from the inner ring. This structure represents the protein backbone of the pancreatic porosome complex. Bar=30 nm. **(b)** EM of the isolated porosome complex cut out from figure a, and **(c)** an outline of the structure presented for clarity. **(d-f)** AFM micrograph of an isolated porosome complex in physiological buffer solution. Bar=30 nm. Note the structural similarity of the complex when imaged either by EM **(g)** or AFM **(h)**. The EM and AFM micrographs are superimposable **(i)**. (From Ref 40).

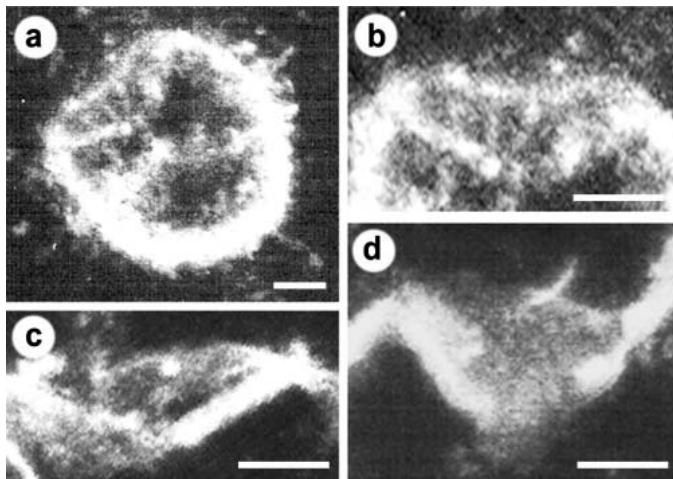


**Figure 13.** Electron micrographs of reconstituted porosome complex into liposomes, demonstrate a cup-shaped basket-like morphology. **(a)** A 500-nm vesicle with an incorporated porosome complex is shown. Note the spokes in the complex. The reconstituted complex at higher magnification is shown in **b-d**. Bar=100 nm. (From Ref 42).

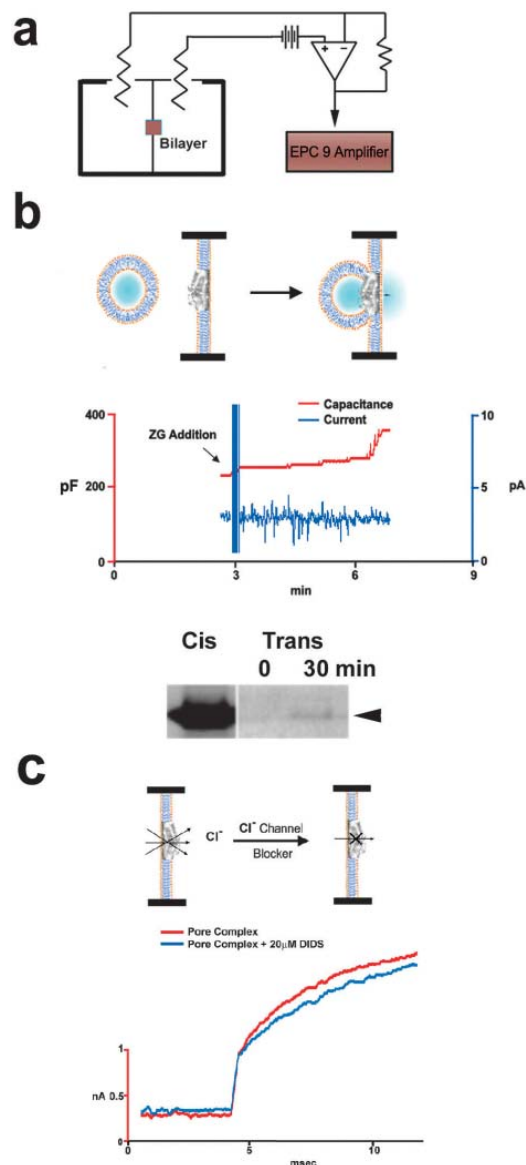


**Figure 14.** Functional reconstitution of the pancreatic porosome complex. **(a)** Schematic drawing of the EPC9 bilayer setup for electrophysiological measurements. **(b)** Zymogen granules (ZGs) added to the cis compartment (left) of the bilayer fuse with the reconstituted porosomes, as demonstrated by the increase in capacitance (red trace) and current (blue trace) activities, and a concomitant time dependent release of amylase to the trans compartment of the bilayer. The movement of amylase from the cis to the trans compartment in the EPC9 setup was determined by Western blot analysis of the contents in the cis and the trans chamber over time. **(c)** Electrical measurements in the presence and absence of chloride ion channel blocker DIDS, demonstrate the presence of chloride channels in association with the complex, and its requirement in porosome function. (From Ref 42).

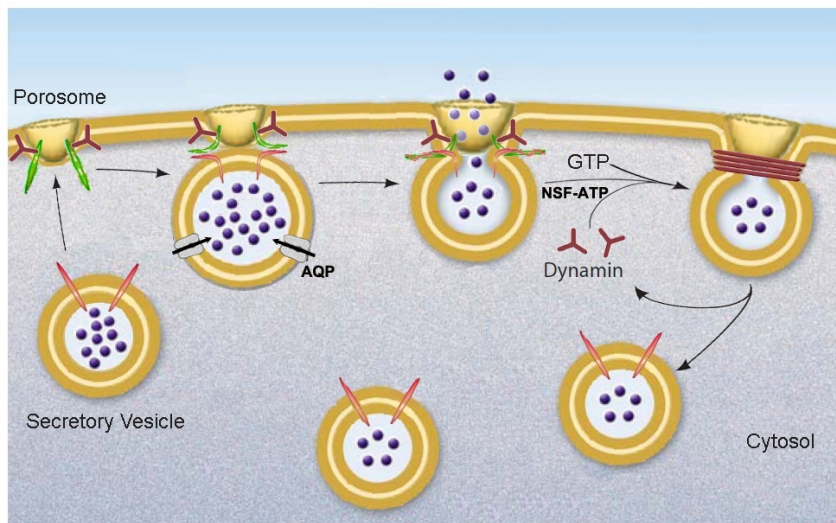


**Figure 15.** Schematic diagram depicting the transient docking and fusion of secretory vesicles at the porosome base in the cell plasma membrane, increase in turgor pressure of secretory vesicles via the entry of water and ions through water channels called aquaporins (AQP) and ion channels, expulsion of vesicular contents via the porosome to the outside, and the dissociation of the partially empty secretory vesicles from the porosome complex at the cell plasma membrane. (From Ref 47).

Immunoprecipitation studies using SNAP-23 specific antibody on solubilized pancreatic plasma membrane fractions demonstrate the isolation of the porosome complex as assessed both structurally (**Figure 12,13**) and functionally (**Figure 14**) (40). Furthermore, immunochemical characterization of the pancreatic porosome complex demonstrates the presence of SNAP-23, syntaxin 2, actin, fodrin, vimentin, chloride channels CLC2 and CLC3, calcium channels  $\beta 3$  and  $\alpha 1c$ , and the SNARE regulatory protein NSF, among other proteins (35,36).

Transmission electron micrographs of pancreatic porosomes reconstituted into liposomes, exhibit a 150–200 nm cup-shaped basket-like morphology (**Figure 13**), similar to its native structure observed in cells and when co-isolated with ZG preparation (40). To test the functionality of the immunoprecipitated porosome complex, purified porosomes obtained from exocrine pancreas have been reconstituted in the lipid membrane of the electrophysiological bilayer setup, and exposed to isolated ZGs (**Figure 14**). Electrical activity of the porosome-reconstituted membrane as well as the transport of vesicular contents from the *cis* to the *trans* compartments of the bilayer

chambers when monitored, demonstrate that the lipid membrane-reconstituted porosomes are indeed functional, since in the presence of calcium, isolated secretory vesicles dock and fuse to transfer intravesicular contents from the *cis* to the *trans* compartment of the bilayer chamber (**Figure 14**). ZGs fusion and content release through the reconstituted porosome is demonstrated by the increase in capacitance and conductance, and a time-dependent transport of the ZG enzyme amylase from *cis* to the *trans* compartment of the bilayer chamber. Amylase is detected using immunoblot analysis of the buffer in the *cis* and *trans* compartments of the bilayer chambers. Chloride channel activity present in the porosome complex is critical to porosome function, since the chloride channel blocker DIDS is inhibitory to the reconstituted porosome (**Figure 14**). Recent studies (28) demonstrate the interaction between the cystic fibrosis transmembrane conductance regulator (CFTR) and the porosome complex in human airways epithelia. CFTR being a chloride selective ion channel, its role on the quality of mucus secretion via the porosome complex at the cell plasma membrane of the airways epithelia is implicated from the study. Similarly in cystic fibrosis,

dysfunction of the CFTR is known to reduce secretory activity of the tubular duct cells (25) which leads to blockage of the ductal system and eventual fibrosis of the entire gland. This is just one examples of diseases resulting from alterations in a porosome-associated proteins.

In summary, these studies demonstrate that the power and scope of the AFM enabled the discovery of the porosome (27, 57, 67), first in acinar cells of the exocrine pancreas, and later in other cell types including neurons. Porosomes are permanent supramolecular lipoprotein structures at the cell plasma membrane in pancreatic acinar cells, where membrane-bound secretory vesicles called zymogen granules or ZGs transiently dock and fuse to release intravesicular contents to the outside. A schematic drawing (33, 47) of porosome-mediated fractional discharge of intravesicular contents during cell secretion is presented in figure 15. As opposed to the complete merger of secretory vesicles at the cell plasma membrane (a all or none mechanism), the porosome complex prevents secretory vesicle

collapse at the cell plasma membrane and provides precise regulation of content release during secretion. Whether secretion involves the docking and fusion of a single vesicle or compound exocytosis where a docked vesicle may have a number of vesicles fused to it, the porosome would provides specificity and regulation of content release. It is speculated that following partial discharge of intravesicular contents, the partially empty vesicle may undergo one to several docking-fusion-release cycles until empty of contents, prior to recycling through endosome-Golgi and or the endosome-lysosome-Golgi pathway. A better understand the molecular structure and control of the porosome complex is required before therapeutic targets could be developed to help ameliorate its secretory dysfunction. Therefore understanding the distribution of constituent proteins within the complex is required, which is in progress using small angle X-ray solution scattering (43), chemical cross linking followed my mass spectrometry (47), immuno-EM, immuno-AFM, and single particle cryo electron tomography.

**Acknowledgement:** The work described in this manuscript was supported by grants from the NIH R01 DK56212 and NS39918 to BPJ.

### 3. References

1. **Alexander, S., Hellemans, L., Marti, O., Schneir, J., Elings, V., Hansma, P. K.** An atomic resolution atomic force microscope implemented using an optical lever. *J. Appl. Phys.* 65, 164–167, 1989.
2. **Almers, W., Tse, F. W.** Transmitter release from synapses: does a preassembled fusion pore initiate exocytosis? *Neuron*. 4: 813-818, 1990. [PMID: 1972885](#)
3. **Aravanis AM, Pyle JL, Tsien RW.** Single synaptic vesicles fusing transiently and successively without loss of identity. *Nature* 423: 643–647, 2003. [PMID: 12789339](#)
4. **Bennett, M.K., Calakos, N., Scheller, R.H.** Syntaxin: A synaptic protein implicated in docking of synaptic vesicles at presynaptic active zones. *Science* 257:255-259, 1992. [PMID: 1321498](#)
5. **Binnig, G., Quate, C. F., Gerber, C. H.** Atomic force microscope. *Phys. Rev. Lett.* 56, 930–933, 1986. [PMID: 10033323](#)
6. **Brunger, A. T., Weninger, K., Bowen, M. & Chu, S.** Single-molecule studies of the neuronal SNARE fusion machinery. *Annu. Rev. Biochem.* 78: 903–928, 2009. [PMID: 19489736](#)
7. **Ceccarelli, B., Hurlbut, W.P., Mauro, A.** Turnover of transmitter and synaptic vesicles at the frog neuromuscular junction. *Journal of Cell Biology* 57: 499-524, 1973. [PMID: 4348791](#)
8. **Chapman, E. R.** How does synaptotagmin trigger neurotransmitter release? *Annu. Rev. Biochem.* 77: 615–641, 2008. [PMID: 18275379](#)
9. **Chen, Z-H., Lee, J-S., Shin, L., Cho, W-J., Jena, B.P.** Involvement of  $\beta$ -adrenergic receptor in synaptic vesicle swelling and implication in neurotransmitter release. *J. Cell. Mol. Med.* 15: 572-576, 2011. [PMID: 20132410](#)
10. **Cho, S.-J., Cho, J., Jena, B.P.** Number of secretory vesicles remain unchanged following exocytosis. *Cell Biol. Int.* 26(1):29-33, 2002. [PMID: 11779218](#)

11. **Cho, S.-J., Jeftinija, K., Glavaski, A., Jeftinija, S., Jena, B.P., L.L. Anderson.** Structure and dynamics of the fusion pores in live GH-secreting cells revealed using atomic force microscopy. *Endocrinology* 143: 1144-1148, 2002. [PMID: 11861542](#)
12. **Cho, S.-J., M. Kelly, M., Rognlien, K.T., Cho, J.A., Horber, J.K.H., Jena, B.P.** SNAREs in opposing bilayers interact in a circular array to form conducting pores. *Biophys. J.* 83: 2522-2527, 2002. [PMID: 12414686](#)
13. **Cho, S.-J., Quinn, A.S., Stromer, M.H., Dash, S., Cho, J., Taatjes, D.J., Jena, B.P.** Structure and dynamics of the fusion pore in live cells. *Cell Biol. Int* 26: 35-42, 2002. [PMID: 11779219](#)
14. **Cho, S.-J., Sattar, A.K.M., Jeong, E.-H., Satchi, M., Cho, J., Dash, S., Mayes, M.S., Stromer, M.H., Jena, B.P.** Aquaporin 1 regulates GTP-induced rapid gating of water in secretory vesicles. *Proc. Natl. Acad. Sci. USA.* 99: 4720-4724, 2002. [PMID: 11917120](#)
15. **Cho, S.-J., Wakade, A., Pappas, G.D., Jena, B.P.** New structure involved in transient membrane fusion and exocytosis. *New York Academy of Science Annals*, 971: 254-256, 2002. [PMID: 12438127](#)
16. **Cho, W.J., Lee, J.-S., Ren, G., Zhang, L., Shin, L., Manke, C.W., Potoff, J., Kotaria, N., Zhvania, M.G., Jena, B.P.** Membrane-directed molecular assembly of the neuronal SNARE complex. *J. Cell. Mol. Med.* 15: 31-37, 2011. [PMID: 20716122](#)
17. **Cho, W.-J., Jeremic, A., Jena, B. P.** Size of supramolecular SNARE complex: membrane-directed self-assembly. *J. Am. Chem. Soc.* 127: 10156-10157, 2005. [PMID: 16028912](#)
18. **Cho, W.-J., Jeremic, A., Rognlien, K. T., Zhvania, M.G., Lazrishvili, I., Tamar, B., Jena, B.P.** Structure, isolation, composition and reconstitution of the neuronal fusion pore. *Cell Biol. Int.* 28: 699-708, 2004. [PMID: 15516328](#)
19. **Cook, J.D., Cho, W.J., Stemmler, T.L., Jena, B.P.** Circular dichroism (CD) spectroscopy of the assembly and disassembly of SNAREs: the proteins involved in membrane fusion in cells. *Chem. Phys. Lett.* 462: 6-9, 2008. [PMID: 19412345](#)
20. **Craciun C, Barbu-Tudoran L.** Identification of new structural elements within 'porosomes' of the exocrine pancreas: a detailed study using high-resolution electron microscopy. *Micron* 44: 137-142, 2013. [PMID: 22819153](#)
21. **Diao, J., Ishitsuka, Y. & Bae, W. R.** Single-molecule FRET study of SNARE-mediated membrane fusion. *Biosci. Rep.* 31: 457-463, 2011. [PMID: 21919892](#)
22. **Drescher DG, Cho WJ, Drescher MJ.** Identification of the porosome complex in the hair cell. *Cell Biol Int Rep* 18: 31-34, 2011. [PMID: 22348194](#)
23. **Els Hennawy WW.** Image processing and numerical analysis approaches of porosome in mammalian pancreatic acinar cell. *J American Sci* 6: 835-843, 2011.
24. **Fasshauer, D. & Margittai, M.** A Transient N-terminal interaction of SNAP-25 and syntaxin nucleates SNARE assembly. *J. Biol. Chem.* 279: 7613-7621, 2004. [PMID: 14665625](#)
25. **Gray, M.A, Winpenny, J.P, Verdon B, McAlroy, H, Argent, B.E.** Chloride channel and cystic fibrosis of the pancreas. *Biosci. Rep.* 15(6):531-541, 1995. [PMID: 9156582](#)
26. **Hammel I, Meilijson I.** Function suggests nano-structure: electrophysiology supports that granule membranes play dice. *J R Soc Interface* 9: 2516-2526, 2012. [PMID: 22628211](#)
27. **Hörber, J. K. H., Miles, M. J.** Scanning probe evolution in biology. *Science* **302**, 1002-1005, 2003. [PMID: 14605360](#)
28. **Hou, X., Lewis, K.T., Wu, Q., Wang, S., Chen, X., Flack, A., Mao, G., Taatjes, D.J., Sun, F., Jena, B.P.** Proteome of the porosome complex in human airways epithelia: Interaction with the cystic fibrosis transmembrane conductance regulator (CFTR). *Journal of Proteomics* 96:82-91, 2014. [PMID: 24220302](#)
29. **Hui, E., Johnson, C. P, Yao, J, Dunning, F. M, Chapman, E. R.** Synaptotagmin-mediated bending of the target membrane is a critical step in Ca<sup>2+</sup>-regulated fusion. *Cell* 138: 709-721, 2009. [PMID: 19703397](#)
30. **Issa, Z., Manke, C.W., Jena, B.P. Potoff, J.J.** Ca<sup>2+</sup> bridging of apposed phospholipid bilayer *J. Phys. Chem.* 114: 13249-13254, 2010. [PMID: 20836527](#)
31. **Jahn, R. & Scheller, R. H.** SNAREs—engines for membrane fusion. *Nature Rev. Mol. Cell Biol.* 7: 631-643, 2006. [PMID: 16912714](#)
32. **Japaridze NJ, Okuneva VG, Qsovreli MG, Surmava AG, Lordkipanidze TG, Kiladze MT, Zhvania MG.** Hypokinetic stress and neuronal porosome complex in the rat brain: The electron microscopic study. *Micron* 43: 948-953, 2012. [PMID: 22571877](#)
33. **Jena, B. P.** Porosome: the secretory portal. *Exp. Biol. Med.* 237: 748-757, 2012. [PMID: 22859740](#)
34. **Jena, B. P. ,Schneider, S. W., Geibel, J. P., Webster, P., Oberleithner, H., and Sritharan, K. C.** Gi regulation of secretory vesicle swelling examined by atomic force microscopy. *Proc. Natl. Acad. Sci, USA.* 94: 13317-13322, 1997. [PMID: 9371843](#)
35. **Jena, B. P., Cho, S.-J, Jeremic, A., Stromer, M.H., Abu-Hamdah, R.** Structure and composition of the fusion pore. *Biophys. J.* 84: 1337-1343, 2003. [PMID: 12547814](#)

36. **Jena, B.P.** NanoCellBiology of Secretion: Imaging its Cellular and Molecular Underpinnings. *Springer Briefs in Biological Imaging* 1: 1-70, 2012.
37. **Jeremic, A., Cho, W-J, Jena, B.P.** Membrane fusion: what may transpire at the atomic level. *J. Biol. Phys. & Chem.* 4: 139-142, 2004.
38. **Jeremic, A., Cho, W-J., Jena, B.P.** Involvement of water channels in synaptic vesicle swelling. *Exp. Biol. Med.* 230: 674-680, 2005. [PMID: 16179736](#)
39. **Jeremic, A., Kelly, M., Cho, J-H., Cho, S-J., Horber, J.K.H., Jena, B.P.** Calcium drives fusion of SNARE-apposed bilayers. *Cell Biol. Int.* 28: 19-31, 2004. [PMID: 14759765](#)
40. **Jeremic, A., Kelly, M., Cho, S-J., Stromer, M.H., Jena, B.P.** Reconstituted fusion pore. *Biophys. J.* 85: 2035-2043, 2003. [PMID: 12944316](#)
41. **Jeremic, A., Quinn, A.S., Cho, W-J., Taatjes, D.J., Jena, B.P.** Energy-dependent disassembly of self-assembled SNARE complex: observation at nanometer resolution using atomic force microscopy. *J. Am. Chem. Soc.* 128: 26-27, 2006. [PMID: 16390104](#)
42. **Kelly, M., Cho, W-J., Jeremic, A., Abu-Hamdah, R., Jena, B.P.** Vesicle swelling regulates content expulsion during secretion. *Cell Biol. Int.* 28: 709-716, 2004. [PMID: 15516329](#)
43. **Kovari, L.C., Brunzelle, J.S., Lewis, K.T., Cho, W.J., Lee, J-S., Taatjes, D.J., Jena, B.P.** X-ray solution structure of the native neuronal porosome-synaptic vesicle complex: Implication in neurotransmitter release. *Micron* 56: 37-43, 2014. [PMID: 24176623](#)
44. **Larina O, Bhat P, Pickett JA, Launikonis BS, Shah A, Kruger WA, Edwardson JM, Thorn P.** Dynamic regulation of the large exocytotic fusion pore in pancreatic acinar cells. *Mol Biol Cell.* 18(9):3502-3511, 2007. [PMID: 17596517](#)
45. **Lee, J-S, Cho, W-J., Shin, L., Jena, B. P.** Involvement of cholesterol in synaptic vesicle swelling. *Exp. Biol. Med.* 235: 470-477, 2010. [PMID: 20407079](#)
46. **Lee, J-S, Hou X, Bishop N, Wang S, Flack A, Cho W.J, Chen X, Mao G, Taatjes D.J, Sun F, Zhang K, Jena B.P.** Aquaporin-assisted and ER-mediated mitochondrial fission: a hypothesis. *Micron* 47: 50-58, 2013. [PMID: 23416165](#)
47. **Lee, J-S, Jeremic, A., Shin, L., Cho, WJ., Chen, X., Jena, B.P.** Neuronal Porosome proteome: Molecular dynamics and architecture. *Journal of Proteomics* 75: 3952-3962, 2012. [PMID: 22659300](#)
48. **Martens, S., Kozlov, M. M. & McMahon, H. T.** How synaptotagmin promotes membrane fusion. *Science* 316: 1205–1208, 2007. [PMID: 17478680](#)
49. **Matsuno A, Itoh J, Mizutani A, Takekoshi S, Osamura RY, Okinaga H, Ide F, Miyawaki S, Uno T, Asano S, Tanaka J, Nakaguchi H, Sasaki M, Murakami M.** Co-transfection of EYFP-GH and ECFP-rab3B in an experimental pituitary GH3 cell: a role of rab3B in secretion of GH through porosome. *Folia Histochem Et Cytobiologica* 46, 419-421, 2008. [PMID: 19141391](#)
50. **Misura, K. M., Scheller, R. H. & Weis, W. I.** Three-dimensional structure of the neuronal-Sec1–syntaxin 1a complex. *Nature* 404: 355–362, 2000. [PMID: 10746715](#)
51. **Monck, J.R., Fernandez, J.M.** The exocytotic fusion pore. *Journal of Cell Biology* 119: 1395-1404, 1992. [PMID: 1469040](#)
52. **Okuneva VG, Japaridze ND, Kotaria NT, Zhvania MG.** Neuronal porosome in the rat and cat brain. *Cell & Tissue Biol* 6: 69-72, 2012. [PMID: 22724370](#)
53. **Oyler, G.A., Higgins, G.A., Hart, R.A., Battenberg, E., Billingsley, M., Bloom, F.E., Wilson, M.C.** The identification of a novel synaptosomal-associated protein, SNAP-25, differentially expressed by neuronal subpopulations. *J. Cell Biol.* 109: 3039-3052, 1989. [PMID: 2592413](#)
54. **Paredes-Santos TC, de Souza W, Attias M.** Dynamics and 3D organization of secretory organelles of *Toxoplasma Gondii*. *J Struct Biol* 177: 420-430, 2012. [PMID: 22155668](#)
55. **Pobbati, A. V., Stein, A. & Fasshauer, D.** N- to C-terminal SNARE complex assembly promotes rapid membrane fusion. *Science* 313: 673–676, 2006. [PMID: 16888141](#)
56. **Savigny P, Evans J, McGarth KM.** Cell membrane structures during exocytosis. *Endocrinology* 148: 3863-3874, 2007. [PMID: 17494998](#)
57. **Schneider, S. W., Sritharan, K. C., Geibel, J. P., Oberleithner, H., Jena, B. P.** Surface dynamics in living acinar cells imaged by atomic force microscopy: identification of plasma membrane structures involved in exocytosis. *Proc. Natl. Acad. Sci, USA.* 94: 316-321, 1997. [PMID: 8990206](#)
58. **Shen, J., Tareste, D. C., Paumet, F., Rothman, J. E. & Melia, T. J.** Selective activation of cognate SNAREpins by Sec1/Munc18 proteins. *Cell* 128: 183–195, 2007. [PMID: 17218264](#)
59. **Shin, L., Basi, N., Lee, J-S., Cho, W-J., Chen, Z., Abu-Hamdah, R., Oupicky, D., Jena, B. P.** Involvement of vH<sup>+</sup>-ATPase in synaptic vesicle swelling. *J. Neurosci. Res.* 88: 95-101, 2010. [PMID: 19610106](#)
60. **Shin, L., Cho, W-J., Cook, J., Stemmler, T., Jena, B.P.** Membrane lipids influence protein complex assembly-disassembly. *J. Am. Chem. Soc.* 132: 5596-5597, 2010. [PMID: 20373736](#)

61. **Siksou L, Rostaing P, Lechaire JP, Boudier T, Ohtsuka T, Fejtova A, Kao HT, Greengard P, Gundelfinger ED, Triller A, Marty S.** Three-dimensional architecture of presynaptic terminal cytomatrix. *J Neurosci* 27: 6868–6877, 2007. [PMID: 17596435](#)
62. **Stein, A., Weber, G., Wahl, M. C. & Jahn, R.** Helical extension of the neuronal SNARE complex into the membrane. *Nature* 460: 525–528, 2009. [PMID: 19571812](#)
63. **Südhof, T. C. & Rizo, J.** Synaptic vesicle exocytosis. *Cold Spring Harb. Perspect. Biol.* 3: a005637, 2011. [PMID: 22026965](#)
64. **Südhof, T. C. & Rothman, J. E.** Membrane fusion: grappling with SNARE and SM proteins. *Science* 323: 474–477, 2009. [PMID: 19164740](#)
65. **Südhof, T. C.** The synaptic vesicle cycle. *Annu. Rev. Neurosci.* 27: 509–547, 2004. [PMID: 11144340](#)
66. **Sutton, R.B., Fasshauer, D., Jahn, R., Brunger, A.T.** Crystal structure of a SNARE complex involved in synaptic exocytosis at 2.4 Å resolution. *Nature.* 395: 347–353, 1998. [PMID: 9759724](#)
67. **Taatjes, D.J., Rand, J.H., Jena, B.P.** Atomic force microscopy: high resolution dynamic imaging of cellular and molecular structure in health and disease. *J. Cell Physiol.* 228:1949-1955, 2013. [PMID: 23526453](#)
68. **Taraska JW, Perrais D, Ohara-Imaizumi M, Nagamatsu S, Almers W.** Secretory granules are recaptured largely intact after stimulated exocytosis in cultured endocrine cells. *Proc Natl Acad Sci USA* 100: 2070–2075, 2003. [PMID: 12538853](#)
69. **Thorn P, Fogarty KE, Parker I.** Zymogen granule exocytosis is characterized by long fusion pore openings and preservation of vesicle lipid identity. *Proc Natl Acad Sci USA* 101: 6774–6779, 2004. [PMID: 15090649](#)
70. **Trimble, W.S., Cowan, D.W., Scheller, R.H.** VAMP-1: A synaptic vesicle-associated integral membrane protein. *Proc. Natl. Acad. Sci. USA.* 85: 4538-4542, 1988. [PMID: 3380805](#)
71. **Wang, S., Lee, J-S., Bishop, N., Jeremic, A., Cho, WJ., Chen, X., Mao, G., Taatjes, D.J., Jena, B.P.** 3D organization and function of the cell: Golgi budding and vesicle biogenesis to docking at the porosome complex. *Histochem. Cell Biol.* 137: 703-718, 2012. [PMID: 22527693](#)
72. **Weber, T., Zemelman, B.V., McNew, J.A., Westerman, B., Gmachl, M., Parlati, F., Söllner, T.H., Rothman, J.E.** SNAREpins: minimal machinery for membrane fusion. *Cell.* 92: 759-772, 1998. [PMID: 9529252](#)
73. **Wickner, W. & Schekman, R.** Membrane fusion. *Nature Struct. Mol. Biol.* 15: 658–664, 2008. [PMID: 18618939](#)
74. **Yao, J., Gaffaney, J. D., Kwon, S. E. & Chapman, E. R.** Doc2 is a Ca<sup>2+</sup> sensor required for asynchronous neurotransmitter release. *Cell* 147: 666–677, 2011. [PMID: 22036572](#)
75. **Zhao, D., Lulevich, V., Liu, F., Liu, G.** Applications of atomic force microscopy in biophysical chemistry. *J. Phys. Chem. B.* 114: 5971-5982, 2010. [PMID: 20405961](#)